

---

# SpectralKD: Understanding and Optimizing Vision Transformer Distillation through Spectral Analysis

---

Huiyuan Tian<sup>1</sup> Bonan Xu<sup>2</sup> Shijian Li<sup>1</sup> Gang Pan<sup>1</sup>

## Abstract

Knowledge distillation effectively reduces model complexity while improving performance, yet the underlying knowledge transfer mechanisms remain limited understood. We propose novel spectral analysis methods and guidelines to optimize distillation, making the knowledge transfer process more interpretable. Our analysis reveals that CaiT models concentrate information in their first and last few layers, informing optimal layer selection for feature map distillation. Surprisingly, we discover that Swin Transformer and CaiT exhibit similar spectral encoding patterns despite their architectural differences, enhancing our understanding of transformer architectures and leading to improved feature map alignment strategies. Based on these insights, we introduce a simple yet effective spectral alignment method named SpectralKD. Experimental results demonstrate that following our guidelines enables SpectralKD to achieve state-of-the-art performance (DeiT-Tiny: +5.2%, Swin-Tiny: +1.4% in ImageNet-1k Top-1 accuracy). Furthermore, through spectral analysis of student models trained with and without distillation, we show that distilled models mirror spectral patterns of their teachers, providing a new lens for interpreting knowledge distillation dynamics. Our code, pre-trained models, and experimental logs will be made publicly available.

## 1. Introduction

Knowledge distillation, first introduced by Hinton et al. (Hinton, 2015), is an effective model compression technique that transfers knowledge from a complex teacher model to a simpler student model. This method has demonstrated

remarkable success in various domains (Rusu et al., 2015; Joshi et al., 2024), including but not limited to computer vision (Wang et al., 2024; Li et al., 2024; Fan et al., 2024), natural language processing (Sanh, 2019; Sun et al., 2019; Jiao et al., 2019; Tang et al., 2019; Gu et al., 2024), and multimodal learning (Wang et al., 2020; Li et al., 2021; Radevski et al., 2023; Li et al., 2023; Shen et al., 2023).

The field encompasses two primary approaches: logits distillation and feature distillation. Logits distillation, the original formulation, aims to transfer knowledge by having the student model mimic the output probabilities of the teacher. This was initially proposed using Kullback-Leibler divergence (Hinton, 2015), and has since been expanded to include label smoothing (Müller et al., 2019), label decoupling (Zhao et al., 2022), adaptive probability reweighting (Xu et al., 2020; Zhou et al., 2021; Niu et al., 2022), and logits standardization (Sun et al., 2024).

Feature distillation, first introduced by FitNets (Romero et al., 2014), takes a different approach by aligning intermediate representations between teacher and student networks. This has sparked numerous innovations in feature matching strategies: attention transfer (Zagoruyko & Komodakis, 2016; Shu et al., 2021; Fan et al., 2024), contrastive learning (Tian et al., 2019), and correlation congruence (Chen et al., 2021). Recent advances include both fixed transformation operators (Kim et al., 2018; Huang et al., 2020; Hao et al., 2022; Miles et al., 2024) and learnable projectors (Jang et al., 2019; Miles & Mikolajczyk, 2024) to bridge the dimensional gap between teacher and student features.

Understanding the internal mechanisms of knowledge transfer between teacher and student models is essential for developing trustworthy models with high performance, interpretability, and generalization capabilities. Recent theoretical analyses (Huang et al., 2021; Ji et al., 2021; Beyer et al., 2022; Chandrasegaran et al., 2022; Allen-Zhu & Li, 2023; Zeng et al., 2024) have provided valuable insights: information-theoretic perspectives (Phuong & Lampert, 2019; Miles et al., 2021), statistical learning frameworks (Menon et al., 2021).

In this paper, we propose SpectralKD, a novel framework that brings theoretical insights and practical improvements

---

<sup>1</sup>College of Computer Science and Technology, Zhejiang University, NO. 38 Zheda Road, Xihu District, Hangzhou 310027, China <sup>2</sup>School of Aeronautics and Astronautics, Zhejiang University, NO. 38 Zheda Road, Xihu District, Hangzhou 310027, China. Correspondence to: Shijian Li <shijianli@zju.edu.cn>.

to vision transformer distillation through spectral analysis. Our work makes the following key contributions:

First, we introduce a principled spectral analysis methodology that reveals how information flows through transformer networks. By examining the frequency domain characteristics of feature maps, we discover that transformer models exhibit distinct spectral patterns across different layers, a finding that provides new insights into their internal representations and guides optimal layer selection for distillation. Our frequency-domain approach offers a unique perspective on information encoding.

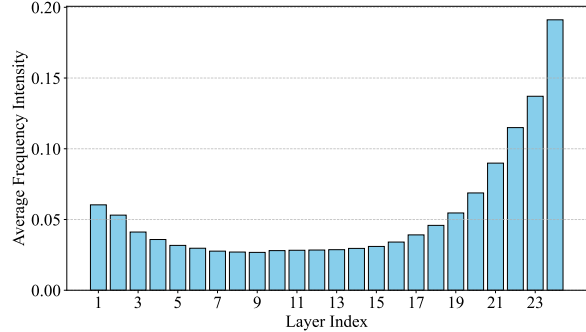
Second, we uncover a surprising architectural insight: despite fundamental differences in design, both hierarchical (Swin Transformer (Liu et al., 2021)) and uniform (CaiT (Touvron et al., 2021b)) architectures demonstrate remarkably similar spectral encoding patterns. This observation not only enhances our understanding of transformer architectures but also leads to more effective feature alignment strategies during distillation. This unexpected finding suggests fundamental principles in how transformers process information.

Third, we leverage these insights to develop SpectralKD, a spectral alignment method that achieves state-of-the-art performance. Our approach demonstrates significant improvements over existing methods: DeiT-Tiny achieves an improvement of 5.2%, and Swin-Tiny shows a 1.4% gain in ImageNet-1k Top-1 accuracy compared to their respective baselines. Through careful analysis of student models trained with and without distillation, we show that successfully distilled models mirror the spectral characteristics of their teachers, providing a new perspective on knowledge transfer dynamics.

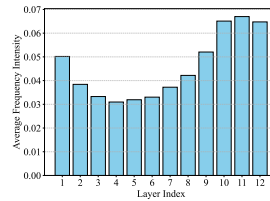
Our spectral analysis framework opens new avenues for understanding and optimizing transformer architectures. Beyond immediate performance gains, it offers a theoretical foundation for analyzing knowledge distillation, potentially influencing the design of more efficient architectures and training strategies. While previous works have primarily focused on empirical improvements, our approach bridges the gap between theoretical understanding and practical performance. Extensive experiments demonstrate that our method not only advances the state-of-the-art in vision transformer distillation but also provides valuable insights into the nature of knowledge transfer in deep neural networks.

## 2. Spectral Analysis for Knowledge Distillation

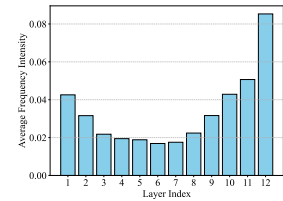
We introduce a novel spectral analysis method to enhance the interpretability of knowledge distillation in vision transformers. Our approach provides quantitative insights into information flow across network layers, offering principled guidance for knowledge distillation. The analytical frame-



(a) CaiT-S24 (teacher).



(b) DeiT-T without distillation.



(c) DeiT-T by SpectralKD.

Figure 1. Layer-wise frequency intensity analysis ( $\ell(\mathbf{X})$ ) across network depths. Comparison between CaiT-S24 (teacher), vanilla DeiT-Tiny (baseline), and DeiT-Tiny trained with our SpectralKD approach. The analysis reveals how SpectralKD helps the student model better mimic the spectral characteristics of teacher models, particularly in information-rich layers. Both CaiT-S24 and baseline DeiT-Tiny checkpoints are from the timm library (Wightman, 2019).

work consists of two key components: (1) a layer-wise frequency intensity measure that identifies optimal layers for distillation, and (2) an intra-layer spectral distribution analysis that guides the feature alignment process. Unlike previous approaches that rely on empirical selection of distillation layers, our method provides a theoretically grounded approach for analyzing and optimizing the distillation process.

### 2.1. Analysis Method

Consider a batch of intermediate feature maps  $\mathbf{X} \in \mathbb{R}^{B \times C \times H \times W}$  from a given layer, where  $B$  is the batch size,  $C$  is the number of channels, and  $H$  and  $W$  denote the spatial height and width, respectively. We apply the one-dimensional Fast Fourier Transform (FFT) along the channel dimension to map these feature maps from the real domain  $\mathbb{R}$  to the complex domain  $\mathbb{C}$ . The transformation is mathematically expressed as:

$$\mathcal{F}(\mathbf{X}) = \text{FFT}(\mathbf{X}), \quad (1)$$

where FFT indicates the FFT applied independently to each channel. This operation involves performing  $B \times H \times W$

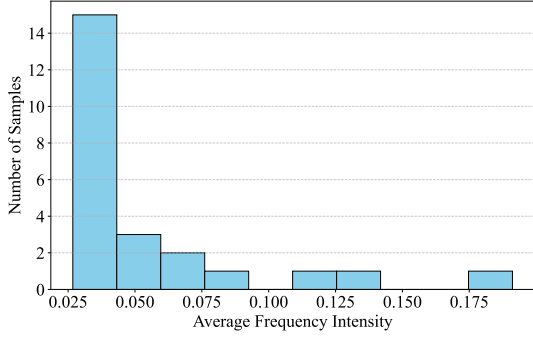


Figure 2. Histogram of layer-wise frequency intensities ( $\ell(\mathbf{X})$ ) in CaiT-S24. The distribution is highly skewed, with a majority of layers showing low spectral magnitudes and only a few layers exhibiting significantly higher information content, suggesting potential critical layers for knowledge distillation.

one-dimensional FFTs on vectors of length  $C$ .

After obtaining the frequency domain representation  $\mathcal{F}(\mathbf{X}) \in \mathbb{C}^{B \times C \times H \times W}$  of the feature maps, we compute the magnitude spectrum of each element in the FFT results as follows:

$$\mathbf{A}(\mathbf{X}) = \sqrt{\text{Re}^2(\mathcal{F}(\mathbf{X})) + \text{Im}^2(\mathcal{F}(\mathbf{X}))}, \quad (2)$$

where  $\text{Re}(\mathcal{F}(\mathbf{X}))$  and  $\text{Im}(\mathcal{F}(\mathbf{X}))$  represent the real and imaginary components of  $\mathcal{F}(\mathbf{X})$ , respectively. The resulting tensor  $\mathbf{A}(\mathbf{X})$  is a real-valued tensor in  $\mathbb{R}^{B \times C \times H \times W}$ .

Next, we compute the average magnitude spectrum by aggregating over the batch size  $B$  and the spatial dimensions  $H$  and  $W$ . This yields an average frequency spectrum for each channel:

$$\mathbf{S}(\mathbf{X}) = \frac{1}{B \times H \times W} \sum_{b=1}^B \sum_{h=1}^H \sum_{w=1}^W \mathbf{A}(\mathbf{X}). \quad (3)$$

Each element in the average frequency spectrum  $\mathbf{S}(\mathbf{X}) \in \mathbb{R}^C$  represents the spectral intensity at a specific frequency, which can be interpreted as the information intensity in the context of information theory (Ash, 2012). Thus,  $\mathbf{S}(\mathbf{X})$  provides insights into the encoding characteristics of neural networks in the spectral domain.

To quantify the overall frequency intensity of a model, we further average the spectral magnitudes across the channel dimension, resulting in a scalar value:

$$\ell(\mathbf{X}) = \frac{1}{C} \sum_{c=1}^C \mathbf{S}(\mathbf{X}), \quad (4)$$

where  $\ell(\mathbf{X})$  represents the average frequency intensity for the feature map of a single layer or stage in the model. The

layer-wise intensity measure  $\ell(\mathbf{X})$  serves as a proxy for the information complexity at each network depth. Higher intensity values typically indicate layers that capture more sophisticated feature representations, making them potential candidates for focused distillation.

When extended to multiple layers or stages, this provides a set of frequency intensity values:

$$L(\mathbf{X}) = \{\ell^{(1)}(\mathbf{X}), \ell^{(2)}(\mathbf{X}), \dots, \ell^{(n)}(\mathbf{X})\}, \quad (5)$$

where  $n$  denotes the total number of layers or stages in the model. The set  $L(\mathbf{X})$  provides a comprehensive profile of how information is processed throughout the network, enabling systematic identification of critical layers for knowledge transfer.

Our spectral analysis provides a hierarchical view of information flow from both layer-wise and channel-wise perspectives. This dual perspective enables more precise and theoretically grounded distillation approaches. Furthermore, we show how teacher models can be analyzed prior to distillation to determine optimal knowledge transfer points, leading to more efficient and effective distillation processes.

## 2.2. Analysis of Teacher Models

Feature-based knowledge distillation presents two fundamental challenges: (1) identifying optimal layers for distillation from an architectural perspective, and (2) aligning features across channel dimensions within feature maps. While hierarchical architectures like Swin Transformer provide natural distillation points at their stage boundaries, the selection of distillation layers for uniform architectures, such as ViT (Dosovitskiy, 2020), CaiT (Touvron et al., 2021b), and DeiT (Touvron et al., 2021a), which comprise sequences of nearly identical Transformer layers, remains an open research question. We address these challenges through comprehensive spectral analysis of representative architectures.

### 2.2.1. SPECTRAL ANALYSIS OF LAYER SELECTION

To systematically investigate optimal layer selection strategies, we analyze the CaiT-S24 model, which consists of 24 Transformer layers, using our proposed spectral framework. Figure 1(a) and 2 present the frequency intensity distribution across layers, computed using Equation 5, through complementary visualizations.

The analysis reveals two key findings: First, as shown in Figure 1(a), the layer-wise average frequency intensities follow a distinctive U-shaped pattern, in which both initial and final layers demonstrate markedly higher spectral intensities, suggesting these layers encode more information-rich representations from an information-theoretic perspective. In contrast, middle layers show notably reduced information content, indicating their potential role in feature trans-

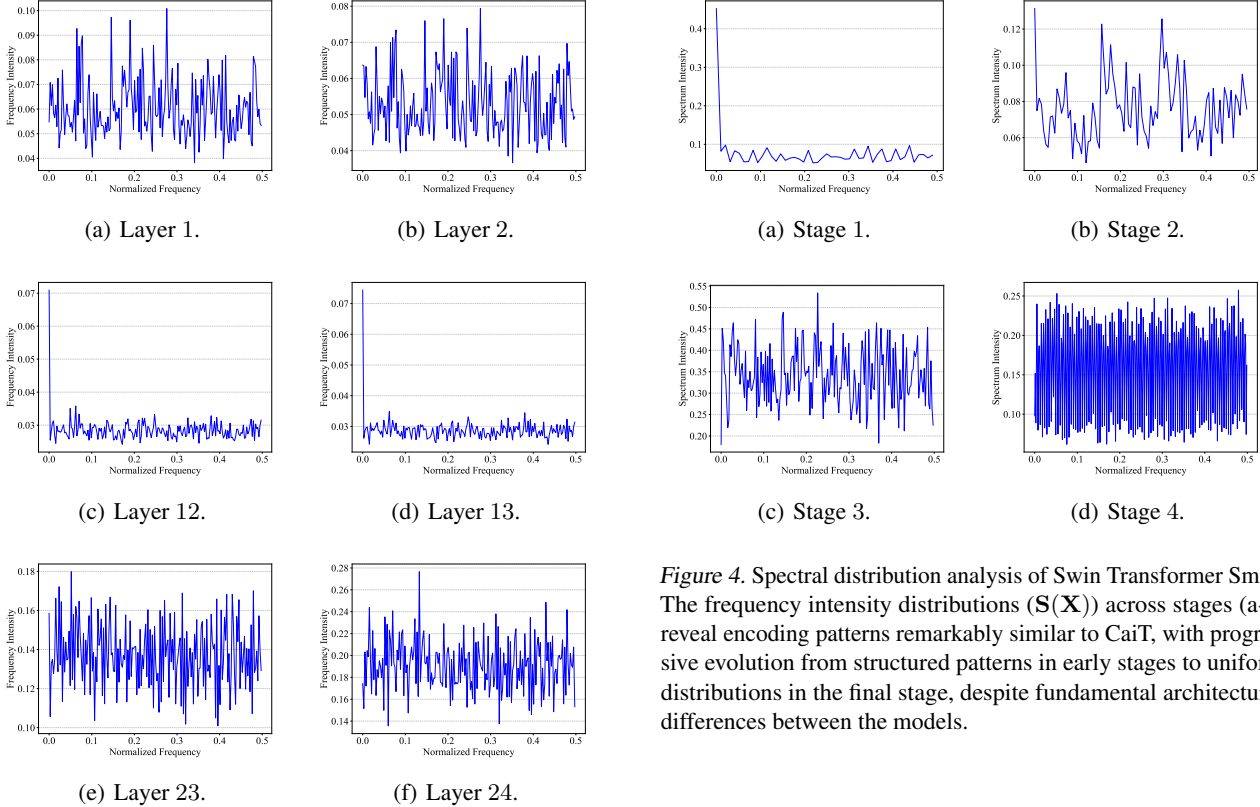


Figure 3. Spectral intensity distributions  $S(\mathbf{X})$  computed using Equation (3) for CaiT-S24 feature maps. The visualization reveals distinct encoding patterns across network depths: uniform distributions in early layers (1-2), exponential decay in middle layers (12-13), and high-intensity uniform distributions in final layers (23-24).

formation rather than information encoding. Second, the histogram in Figure 2 demonstrates a highly skewed distribution of spectral magnitudes, where most layers exhibit relatively low magnitudes while a select few layers show significantly higher values.

### 2.2.2. FEATURE MAP DISTRIBUTION ANALYSIS

We further examine the spectral distribution of information (computed by Equation 3) within individual feature maps across different network depths. Figure 3 illustrates the per-layer frequency distribution patterns in CaiT-S24, revealing three distinct characteristics across network layers:

1. **Initial layers** (Figures 3(a), 3(b)) exhibit relatively uniform distributions across frequency bands but with moderate intensity, suggesting the preservation of high-frequency detailed features during input processing.
2. **Middle layers** (Figures 3(c), 3(d), layers 12-13) demonstrate substantial decay from low to high frequencies, indicating the extraction of more abstract and smooth features. This characteristic may provide novel insights into generalization capabilities of neural networks.
3. **Final layers** (Figures 3(e), 3(f)) show uniform spectral distributions with high information intensity, suggesting efficient utilization of the channel dimension to encode both high- and low-frequency information before classification.

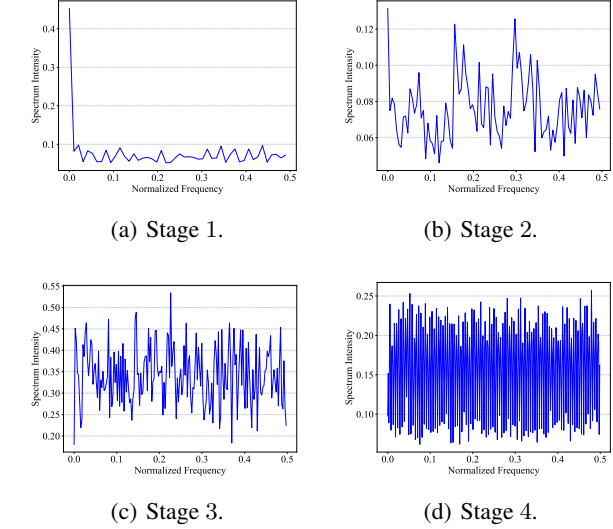


Figure 4. Spectral distribution analysis of Swin Transformer Small. The frequency intensity distributions ( $S(\mathbf{X})$ ) across stages (a-d) reveal encoding patterns remarkably similar to CaiT, with progressive evolution from structured patterns in early stages to uniform distributions in the final stage, despite fundamental architectural differences between the models.

### 2.2.3. CROSS-ARCHITECTURE ANALYSIS

Extending our analysis to different architectures, we examine the Swin Transformer Small model, which represents a fundamentally different architectural design. Figure 4 presents the frequency distribution across its four stages. Surprisingly, despite significant architectural differences, Swin Transformer and CaiT exhibit remarkably similar channel-dimension encoding patterns. A notable observation is the uniform spectral distribution observed in the final stage, a phenomenon that is more characteristic of artificial signals than natural signals, which typically exhibit a decay from low to high frequencies. This finding suggests that deep neural networks actively develop specialized encoding strategies based on abstract features learned in middle layers, rather than merely preserving natural signal characteristics.

#### 2.2.4. IMPLICATIONS FOR KNOWLEDGE DISTILLATION

Our spectral analysis yields several important implications for knowledge distillation: (1) The initial and final layers of uniform architectures like CaiT should be prioritized for distillation, as they encode the most information-rich representations. (2) Feature alignment strategies should account for the varying spectral distributions across network depths, particularly the transition from uniform distributions in early layers to more structured patterns in middle layers. (3) Effective knowledge transfer should maximize the utilization of all channel dimensions, enabling student models to acquire the fine-grained encoding capabilities observed in teacher models.

We validate these findings through empirical experiments in Section 4. The complete spectral distribution analysis across all layers is provided in Appendix A.

### 3. Frequency Alignment Distillation

Our spectral analysis reveals that feature maps in vision transformers contain significant information in both high- and low-frequency components. Based on this observation, we propose a frequency alignment distillation approach that aligns the spectral characteristics between student and teacher networks. By leveraging Fourier transformation, our method captures and aligns both low-frequency components (global structures) and high-frequency components (fine details), enabling more effective knowledge transfer in the feature space.

**Method Overview** Let  $\mathbf{F}_s \in \mathbb{R}^{B \times C_s \times H \times W}$  and  $\mathbf{F}_t \in \mathbb{R}^{B \times C_t \times H \times W}$  denote the feature maps from the student and teacher networks, respectively, where  $B$  is the batch size,  $C_s$  and  $C_t$  denote the number of channels, and  $H, W$  represent the spatial dimensions. Our method processes these feature maps through channel alignment and Fourier transformation before computing the distillation loss.

#### 3.1. Feature Map Processing

**Channel Dimension Alignment** To ensure compatibility between student and teacher feature maps with different channel dimensions, we perform 3-dimensional adaptive average pooling:

$$\mathbf{F}_s = \text{AdaptiveAvgPool}(\mathbf{F}_s) \quad \text{if } C_s > C_t, \quad (6)$$

$$\mathbf{F}_t = \text{AdaptiveAvgPool}(\mathbf{F}_t) \quad \text{if } C_s < C_t. \quad (7)$$

After this operation, both feature maps are in  $\mathbb{R}^{B \times C \times H \times W}$ , where  $C = \min(C_s, C_t)$ . We choose adaptive average pooling over linear projections or attention mechanisms for two reasons: (1) it preserves the spatial structure of features while adjusting channel dimensions, and (2) its simplicity enables clearer analysis of the distillation process. This

design maximizes channel utilization in distillation, following our analysis in Section 2.2 showing that transformer networks encode information across all channels.

**Fourier Transform Application** We apply the 2-dimensional real-valued Fast Fourier Transform (FFT) to each channel of the aligned feature maps along their spatial dimensions:

$$\mathcal{F}(\mathbf{F}_s) = \text{RFFT2}(\mathbf{F}_s), \quad (8)$$

$$\mathcal{F}(\mathbf{F}_t) = \text{RFFT2}(\mathbf{F}_t), \quad (9)$$

where RFFT2 denotes the real-valued 2D FFT operation. Due to the conjugate symmetry property of the Fourier transform of real inputs, the resulting outputs are complex-valued tensors in  $\mathbb{C}^{B \times C \times H \times (W/2+1)}$ , where the width dimension is reduced to  $W/2+1$  while preserving all unique frequency components. To facilitate computation, we decompose these complex-valued results into their real and imaginary components and stack them along a new dimension:

$$\mathcal{F}_{\text{real}}(\mathbf{F}_s) = \text{Re}(\mathcal{F}(\mathbf{F}_s)), \quad (10)$$

$$\mathcal{F}_{\text{imag}}(\mathbf{F}_s) = \text{Im}(\mathcal{F}(\mathbf{F}_s)), \quad (11)$$

$$\mathcal{F}_{\text{stack}}(\mathbf{F}_s) = \text{Stack}(\mathcal{F}_{\text{real}}(\mathbf{F}_s), \mathcal{F}_{\text{imag}}(\mathbf{F}_s)), \quad (12)$$

resulting in tensors of shape  $B \times C \times H \times (W/2+1) \times 2$ . The same operations are applied to the teacher’s feature maps.

#### 3.2. Loss Function Design

**Frequency Alignment Loss** We compute the Mean Squared Error (MSE) loss between the stacked Fourier representations:

$$\mathcal{L}_{\text{FFT}} = \text{MSE}(\mathcal{F}_{\text{stack}}(\mathbf{F}_s) - \mathcal{F}_{\text{stack}}(\mathbf{F}_t)) \quad (13)$$

This loss encourages the student to capture both the global patterns (low frequencies) and local details (high frequencies) present in the teacher’s feature representations.

**Combined Training Objective** We combine our frequency-based loss with traditional knowledge distillation to benefit from both spectral alignment and conventional distillation approaches. The knowledge distillation loss (Hinton, 2015) is defined as:

$$\begin{aligned} \mathcal{L}_{\text{KD}} = & (1 - \alpha) \mathcal{L}_{\text{CE}}(f_s(\mathbf{x}), y) \\ & + \alpha T^2 \mathcal{L}_{\text{KL}} \left( \frac{f_s(\mathbf{x})}{T}, \frac{f_t(\mathbf{x})}{T} \right), \end{aligned} \quad (14)$$

where  $\mathcal{L}_{\text{CE}}$  is the cross-entropy loss between the student’s predictions  $f_s(\mathbf{x})$  and ground truth labels  $y$ , and  $\mathcal{L}_{\text{KL}}$  is the Kullback-Leibler divergence. The temperature  $T$  controls the softness of probability distributions, and  $\alpha$  balances the cross-entropy and KL-divergence terms.

The total loss combines both objectives:

$$\mathcal{L}_{\text{Total}} = \mathcal{L}_{\text{KD}} + \beta \mathcal{L}_{\text{FFT}}, \quad (15)$$

where  $\beta$  is a hyperparameter that controls the contribution of frequency alignment to the overall training objective. This combined loss ensures that the student network learns both the decision boundary and the internal feature representations of the teacher model.

## 4. Experiments

We demonstrate the effectiveness of SpectralKD through comprehensive experiments on image classification tasks. Our empirical results show that our spectral analysis-based guidelines lead to state-of-the-art knowledge distillation performance. This section details our experimental setup, presents comprehensive results, and validates our approach through detailed ablation studies.

### 4.1. Experimental Setup

**Dataset and Models.** We conduct experiments on the ImageNet-1k (Deng et al., 2009) comprising 1.28M training images and 50K validation images across 1,000 classes, using various vision transformer architectures.

**Implementation Details.** We conduct all experiments using 2 NVIDIA RTX 4090 GPUs with batch size set to 256. Training DeiT-Tiny requires approximately 184 GPU hours. Our implementation uses PyTorch and builds upon the timm library (Wightman, 2019) for model architectures and pre-trained weights.

**Student Networks.** We evaluate multiple vision transformer variants as student models, all trained exclusively on ImageNet-1k:

1. DeiT-Tiny and DeiT-Small, trained from scratch following the DeiT settings (Touvron et al., 2021a).
2. Swin Transformer-Tiny, trained from scratch using the original Swin Transformer settings (Liu et al., 2021).

**Teacher Networks.** We employ CaiT and Swin Transformer-Small architectures as teachers, using models pretrained solely on ImageNet-1k (without ImageNet-22k pretraining). We obtain pretrained teacher checkpoints from the timm library.

**Hyperparameters.** For all experiments, we maintain consistent hyperparameters: distillation temperature of 1,  $\alpha = 0.9$ , and  $\beta = 0.2$ .

### 4.2. Results and Analysis

Table 1 presents our ImageNet-1k results for DeiT student models, comparing SpectralKD with state-of-the-art knowl-

edge distillation methods. All experiments use CaiT-S24 (47M parameters) as the teacher model. Following our spectral analysis insights, we apply distillation to the first two and final six layers of both networks. We train DeiT-Tiny for 400 epochs and DeiT-Small for 500 epochs, following the DeiT training protocol (Touvron et al., 2021a) with stochastic depth rate set to 0.

**DeiT-Tiny Results.** Using DeiT-Tiny (5M parameters) as the student model, our method achieves state-of-the-art performance. Starting from a baseline accuracy of 72.2%, SpectralKD significantly improves the performance of model to 77.4% Top-1 accuracy, representing a 5.2% absolute improvement. Notably, our method demonstrates stronger knowledge transfer efficiency compared to the conventional hard distillation baseline (74.5%).

**DeiT-small Results.** For the larger DeiT-Small student (22M parameters), SpectralKD maintains its strong performance. From a baseline accuracy of 79.9%, our method achieves 82.2% Top-1 accuracy, which demonstrates a significant improvement over hard distillation (81.3%), with an absolute gain of 0.9%. This consistent performance across different model scales demonstrates the effectiveness of our frequency-based distillation approach in transferring knowledge from teacher to student networks.

**Swin Transformer Results.** We further evaluate SpectralKD on hierarchical architectures, using Swin Transformer-Small (50M parameters) as teacher and Swin Transformer-Tiny (29M parameters, 81.3% baseline) as student. Table 2 shows that SpectralKD achieves 82.7% Top-1 accuracy, demonstrating a significant 1.4% improvement over baseline model. This strong performance is particularly noteworthy as it demonstrates that our SpectralKD effectively transfers knowledge between hierarchical transformer architectures, which have fundamentally different attention mechanisms and feature hierarchies compared to DeiT models.

### 4.3. Ablation Study

To thoroughly evaluate the effectiveness of our proposed SpectralKD method, we conduct comprehensive ablation studies on ImageNet-1K using DeiT-Tiny as the student model.

Table 3 presents the results of different knowledge distillation configurations. When combining our proposed SpectralKD with soft knowledge distillation, the student model achieves the best performance of 77.4%, surpassing the baseline by 5.2%. This notable improvement validates our hypothesis that incorporating spectral information during knowledge distillation enables more effective transfer of structural knowledge from the teacher to the student. The superior performance of our full model demonstrates that SpectralKD complements traditional knowledge distillation

Table 1. Classification accuracies on ImageNet-1K for DeiT-Tiny and DeiT-Small.

DISTILLATION METHOD	TEACHER	PARAMS	TOP-1 (%)	STUDENT	TOP-1 (%)
-	-	-	-	DEiT-TINY (5M)	72.2
HARD (TOUVRON ET AL., 2021A)	REGNETY-16GF	84M	82.9	DEiT-TINY (5M)	74.5
DEARKD (CHEN ET AL., 2022)	REGNETY-16GF	84M	82.9	DEiT-TINY (5M)	74.8
USKD (YANG ET AL., 2023)	REGNETY-16GF	84M	82.9	DEiT-TINY (5M)	75.0
SRD (MILES & MIKOLAJCZYK, 2024)	REGNETY-16GF	84M	82.9	DEiT-TINY (5M)	77.2
HARD	CAiT-S24	47M	83.4	DEiT-TINY (5M)	74.5
MANIFOLD (HAO ET AL., 2022)	CAiT-S24	47M	83.4	DEiT-TINY (5M)	76.5
MASKEDKD (SON ET AL., 2025)	CAiT-S24	47M	83.4	DEiT-TINY (5M)	75.9
<b>SPECTALKD (OURS)</b>	CAiT-S24	47M	83.4	DEiT-TINY (5M)	<b>77.4</b>
-	-	-	-	DEiT-SMALL (22M)	79.9
HARD (TOUVRON ET AL., 2021A)	REGNETY-16GF	84M	82.9	DEiT-SMALL (22M)	81.2
DEARKD (CHEN ET AL., 2022)	REGNETY-16GF	84M	82.9	DEiT-SMALL (22M)	81.5
USKD (YANG ET AL., 2023)	REGNETY-16GF	84M	82.9	DEiT-SMALL (22M)	80.8
SRD (MILES & MIKOLAJCZYK, 2024)	REGNETY-16GF	84M	82.9	DEiT-SMALL (22M)	82.1
HARD	CAiT-S24	47M	83.4	DEiT-SMALL (22M)	81.3
MANIFOLD (HAO ET AL., 2022)	CAiT-S24	47M	83.4	DEiT-SMALL (22M)	<b>82.2</b>
<b>SPECTALKD (OURS)</b>	CAiT-S24	47M	83.4	DEiT-SMALL (22M)	<b>82.2</b>

Table 2. Classification accuracies on ImageNet-1K for Swin-Tiny. ‡: Pretrained on ImageNet-22K.

DISTILLATION METHOD	TEACHER	PARAMS (M)	TOP-1 (%)	STUDENT	TOP-1 (%)
-	-	-	-	SWIN-TINY (29M)	81.3
KD	SWIN-LARGE ‡	197M	86.3	SWIN-TINY (29M)	81.5
RKD (PARK ET AL., 2019)	SWIN-LARGE ‡	197M	86.3	SWIN-TINY (29M)	81.2
SRRL (YANG ET AL., 2021)	SWIN-LARGE ‡	197M	86.3	SWIN-TINY (29M)	81.5
DIST (HUANG ET AL., 2022)	SWIN-LARGE ‡	197M	86.3	SWIN-TINY (29M)	82.3
SCALEKD (FAN ET AL., 2024)	SWIN-LARGE ‡	197M	86.3	SWIN-TINY (29M)	<b>83.8</b>
MANIFOLD (HAO ET AL., 2022)	SWIN-SMALL	50M	83.2	SWIN-TINY (29M)	82.2
<b>SPECTALKD (OURS)</b>	SWIN-SMALL	50M	83.2	SWIN-TINY (29M)	<b>82.7</b>

Table 3. Ablation study results on ImageNet-1K. DeiT-Tiny serves as the student model.

METHOD	TOP-1 (%)	$\Delta$ (%)
w/o KD	72.2	-
HARD KD	74.5	+2.3
SOFT KD	76.2	+4.0
SOFT KD + SPECTALKD	<b>77.4</b>	<b>+5.2</b>

methods by capturing additional valuable information that is not explicitly represented in either hard or soft predictions.

Table 4 presents the results of different layer matching strategies between CaiT-S24 (teacher) and DeiT-Tiny (student). Three layer matching strategies are investigated: Early-Late matching (combining initial and final teacher layers), Middle matching (using intermediate layers), and our proposed Spectral matching. The Spectral matching strategy, which aligns teacher layers  $\mathcal{T} = \{1, 2, 19, 20, 21, 22, 23, 24\}$  with student layers  $\mathcal{S} = \{1, 2, 7, 8, 9, 10, 11, 12\}$ , achieves the best performance of 77.4% Top-1 accuracy. This result demonstrates that combining early-layer features with high-

level semantic information selected through spectral analysis leads to optimal knowledge transfer.

## 5. Distillation Dynamics

We analyze the knowledge transfer dynamics between teacher and student models through spectral analysis, revealing the underlying mechanisms of information transmission during the distillation process. Our investigation provides novel insights into how the teacher model’s information processing patterns influence student learning.

The spectral intensity of each transformer layer, calculated using Equation (5), serves as a quantitative measure of information processing capacity grounded in information theory. We conduct a comparative analysis across three model configurations: a teacher model (CaiT-S24) achieving 83.4% accuracy, a baseline student model (DeiT-Tiny) without distillation achieving 72.2% accuracy, and our distilled student model achieving 77.4% accuracy. Figure 1 illustrates the layer-wise spectral intensity distributions across these models.

Table 4. Layer matching strategies and corresponding performance on ImageNet-1K between CaiT-S24 (teacher) and DeiT-Tiny (student). †: Spectral analysis-based layer selection as described in Section 2.

MATCHING STRATEGY	TEACHER LAYERS $\mathcal{T}$	STUDENT LAYERS $\mathcal{S}$	TOP-1 (%)
EARLY-LATE	{1, 2, 3, 4, 21, 22, 23, 24}	{1, 2, 3, 4, 9, 10, 11, 12}	77.2
MIDDLE	{4, 5, 6, 7, 8, 9, 10, 11}	{10, 11, 12, 13, 14, 15, 16, 17}	77.0
SPECTRAL †	{1, 2, 19, 20, 21, 22, 23, 24}	{1, 2, 7, 8, 9, 10, 11, 12}	<b>77.4</b>

The teacher model (Figure 1(a)) exhibits characteristic patterns with high intensity in initial feature extraction layers, reduced intensity in middle processing layers, and elevated intensity in final encoding layers. In contrast, the non-distilled student (Figure 1(b)) shows a similar but less pronounced pattern, with weaker differentiation between middle and final encoding layers and fluctuations in the final three layers, indicating less efficient information processing.

Remarkably, the student model trained with our proposed SpectralKD (Figure 1(c)) demonstrates spectral patterns highly similar to the teacher, despite distillation being applied only to the first two and last six layers. This suggests that selective layer distillation influences global model behavior, as intermediate layers naturally adopt teacher-like information processing patterns. The distilled model exhibits enhanced information intensity in encoding layers and reduced redundancy in middle layers compared to the non-distilled baseline, contributing to its 5.2% accuracy improvement.

These findings reveal that larger teacher models may serve as implicit data cleaners during distillation, with students benefiting from the teacher’s superior noise tolerance and robust information processing. The strong correlation between spectral pattern alignment and performance improvement suggests that effective knowledge transfer manifests as the adoption of teacher-like information processing characteristics throughout the network. This understanding has broader implications for unsupervised and self-supervised learning approaches, potentially opening new avenues for automated image information cleaning and efficient model training strategies.

Our analysis provides empirical evidence that successful knowledge distillation involves more than just matching output distributions. It requires the student to develop internal representations that mirror the information processing hierarchy of teacher.

## 6. Conclusion

In this paper, we introduce SpectralKD, a novel framework for understanding and optimizing vision transformer distillation through spectral analysis. Our work makes several key contributions to the field of knowledge distillation.

First, we develop a principled spectral analysis methodology that reveals how information flows through transformer networks, providing theoretical insights into layer selection for distillation. Second, we discover unexpected similarities in spectral encoding patterns between architecturally distinct models. Third, we demonstrate that these theoretical insights translate into practical improvements, with our approach achieving state-of-the-art performance on standard benchmarks.

Our analysis reveal several important findings that extend beyond immediate performance gains. The discovery that successfully distilled students mirror the spectral characteristics of their teachers suggests that effective knowledge transfer involves more than matching output distributions. It requires the development of similar information processing patterns throughout the network. Moreover, the observation of shared spectral patterns across different transformer architectures hints at fundamental principles in how these models process visual information.

## Impact Statement

Looking forward, our work opens several promising directions for future research. The spectral analysis framework could be extended to other network architectures and tasks beyond vision transformers. The observed relationship between spectral patterns and model performance suggests potential applications in neural architecture search and automated model compression. Additionally, our findings about information flow in transformers may inform the design of more efficient architectures that maintain high performance with reduced computational requirements.

The broader impact of this work extends beyond knowledge distillation. Our spectral analysis framework provides a new lens for understanding deep neural networks, potentially influencing how we approach model design, optimization, and analysis. We believe these insights will contribute to the development of more efficient and interpretable deep learning systems.

## References

Allen-Zhu, Z. and Li, Y. Towards understanding ensemble, knowledge distillation and self-distillation in deep learn-

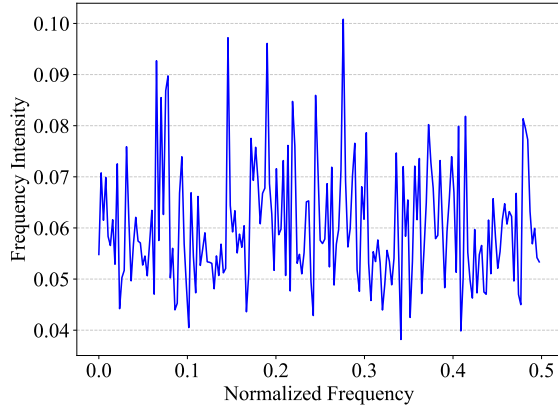


- ing, 2023. URL <https://arxiv.org/abs/2012.09816>.
- Ash, R. B. *Information theory*. Courier Corporation, 2012.
- Beyer, L., Zhai, X., Royer, A., Markeeva, L., Anil, R., and Kolesnikov, A. Knowledge distillation: A good teacher is patient and consistent. In *Proceedings of the IEEE/CVF conference on computer vision and pattern recognition*, pp. 10925–10934, 2022.
- Chandrasegaran, K., Tran, N.-T., Zhao, Y., and Cheung, N.-M. Revisiting label smoothing and knowledge distillation compatibility: What was missing? In *International Conference on Machine Learning*, pp. 2890–2916. PMLR, 2022.
- Chen, P., Liu, S., Zhao, H., and Jia, J. Distilling knowledge via knowledge review. In *Proceedings of the IEEE/CVF conference on computer vision and pattern recognition*, pp. 5008–5017, 2021.
- Chen, X., Cao, Q., Zhong, Y., Zhang, J., Gao, S., and Tao, D. Dearkd: data-efficient early knowledge distillation for vision transformers. In *Proceedings of the IEEE/CVF conference on computer vision and pattern recognition*, pp. 12052–12062, 2022.
- Deng, J., Dong, W., Socher, R., Li, L.-J., Li, K., and Fei-Fei, L. Imagenet: A large-scale hierarchical image database. In *2009 IEEE conference on computer vision and pattern recognition*, pp. 248–255. Ieee, 2009.
- Dosovitskiy, A. An image is worth 16x16 words: Transformers for image recognition at scale. *arXiv preprint arXiv:2010.11929*, 2020.
- Fan, J., Li, C., Liu, X., and Yao, A. Scalekd: Strong vision transformers could be excellent teachers. *arXiv preprint arXiv:2411.06786*, 2024.
- Gu, Y., Dong, L., Wei, F., and Huang, M. Minillm: Knowledge distillation of large language models. In *The Twelfth International Conference on Learning Representations*, 2024.
- Hao, Z., Guo, J., Jia, D., Han, K., Tang, Y., Zhang, C., Hu, H., and Wang, Y. Learning efficient vision transformers via fine-grained manifold distillation. *Advances in Neural Information Processing Systems*, 35:9164–9175, 2022.
- Hinton, G. Distilling the knowledge in a neural network. *arXiv preprint arXiv:1503.02531*, 2015.
- Huang, T., You, S., Wang, F., Qian, C., and Xu, C. Knowledge distillation from a stronger teacher. *Advances in Neural Information Processing Systems*, 35:33716–33727, 2022.
- Huang, Z., Zou, Y., Kumar, B., and Huang, D. Comprehensive attention self-distillation for weakly-supervised object detection. *Advances in neural information processing systems*, 33:16797–16807, 2020.
- Huang, Z., Shen, X., Xing, J., Liu, T., Tian, X., Li, H., Deng, B., Huang, J., and Hua, X.-S. Revisiting knowledge distillation: An inheritance and exploration framework. In *Proceedings of the IEEE/CVF Conference on Computer Vision and Pattern Recognition*, pp. 3579–3588, 2021.
- Jang, Y., Lee, H., Hwang, S. J., and Shin, J. Learning what and where to transfer. In *International conference on machine learning*, pp. 3030–3039. PMLR, 2019.
- Ji, M., Heo, B., and Park, S. Show, attend and distill: Knowledge distillation via attention-based feature matching. In *Proceedings of the AAAI Conference on Artificial Intelligence*, volume 35, pp. 7945–7952, 2021.
- Jiao, X., Yin, Y., Shang, L., Jiang, X., Chen, X., Li, L., Wang, F., and Liu, Q. Tinybert: Distilling bert for natural language understanding. *arXiv preprint arXiv:1909.10351*, 2019.
- Joshi, S., Ni, J., and Mirzasoleiman, B. Dataset distillation via knowledge distillation: Towards efficient self-supervised pre-training of deep networks. *arXiv preprint arXiv:2410.02116*, 2024.
- Kim, J., Park, S., and Kwak, N. Paraphrasing complex network: Network compression via factor transfer. *Advances in neural information processing systems*, 31, 2018.
- Li, J., Selvaraju, R., Gotmare, A., Joty, S., Xiong, C., and Hoi, S. C. H. Align before fuse: Vision and language representation learning with momentum distillation. *Advances in neural information processing systems*, 34: 9694–9705, 2021.
- Li, Y., Wang, Y., and Cui, Z. Decoupled multimodal distilling for emotion recognition. In *Proceedings of the IEEE/CVF Conference on Computer Vision and Pattern Recognition*, pp. 6631–6640, 2023.
- Li, Z., Li, X., Fu, X., Zhang, X., Wang, W., Chen, S., and Yang, J. Promptkd: Unsupervised prompt distillation for vision-language models. In *Proceedings of the IEEE/CVF Conference on Computer Vision and Pattern Recognition*, pp. 26617–26626, 2024.
- Liu, Z., Lin, Y., Cao, Y., Hu, H., Wei, Y., Zhang, Z., Lin, S., and Guo, B. Swin transformer: Hierarchical vision transformer using shifted windows. In *Proceedings of the IEEE/CVF international conference on computer vision*, pp. 10012–10022, 2021.

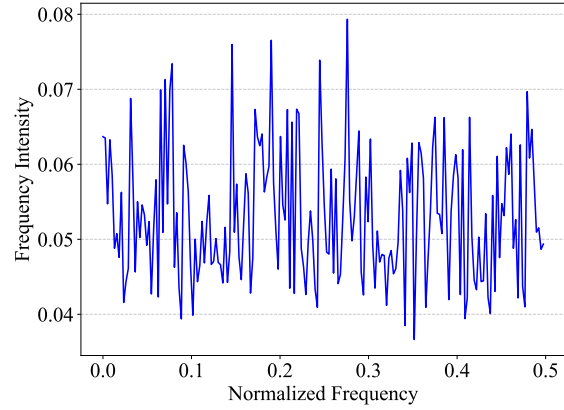
- Menon, A. K., Rawat, A. S., Reddi, S., Kim, S., and Kumar, S. A statistical perspective on distillation. In *International Conference on Machine Learning*, pp. 7632–7642. PMLR, 2021.
- Miles, R. and Mikolajczyk, K. Understanding the role of the projector in knowledge distillation. In *Proceedings of the AAAI Conference on Artificial Intelligence*, volume 38, pp. 4233–4241, 2024.
- Miles, R., Rodriguez, A. L., and Mikolajczyk, K. Information theoretic representation distillation. *arXiv preprint arXiv:2112.00459*, 2021.
- Miles, R., Elezi, I., and Deng, J. Vkd: Improving knowledge distillation using orthogonal projections. In *Proceedings of the IEEE/CVF Conference on Computer Vision and Pattern Recognition*, pp. 15720–15730, 2024.
- Müller, R., Kornblith, S., and Hinton, G. E. When does label smoothing help? *Advances in neural information processing systems*, 32, 2019.
- Niu, Y., Chen, L., Zhou, C., and Zhang, H. Respecting transfer gap in knowledge distillation. *Advances in Neural Information Processing Systems*, 35:21933–21947, 2022.
- Park, W., Kim, D., Lu, Y., and Cho, M. Relational knowledge distillation. In *Proceedings of the IEEE/CVF conference on computer vision and pattern recognition*, pp. 3967–3976, 2019.
- Phuong, M. and Lampert, C. Towards understanding knowledge distillation. In *International conference on machine learning*, pp. 5142–5151. PMLR, 2019.
- Radevski, G., Grujicic, D., Blaschko, M., Moens, M.-F., and Tuytelaars, T. Multimodal distillation for egocentric action recognition. In *Proceedings of the IEEE/CVF International Conference on Computer Vision*, pp. 5213–5224, 2023.
- Romero, A., Ballas, N., Kahou, S. E., Chassang, A., Gatta, C., and Bengio, Y. Fitnets: Hints for thin deep nets. *arXiv preprint arXiv:1412.6550*, 2014.
- Rusu, A. A., Colmenarejo, S. G., Gulcehre, C., Desjardins, G., Kirkpatrick, J., Pascanu, R., Mnih, V., Kavukcuoglu, K., and Hadsell, R. Policy distillation. *arXiv preprint arXiv:1511.06295*, 2015.
- Sanh, V. Distilbert, a distilled version of bert: smaller, faster, cheaper and lighter. *arXiv preprint arXiv:1910.01108*, 2019.
- Shen, Y., Wang, X., Gao, P., and Lin, M. Auxiliary modality learning with generalized curriculum distillation. In *International Conference on Machine Learning*, pp. 31057–31076. PMLR, 2023.
- Shu, C., Liu, Y., Gao, J., Yan, Z., and Shen, C. Channel-wise knowledge distillation for dense prediction. In *Proceedings of the IEEE/CVF International Conference on Computer Vision*, pp. 5311–5320, 2021.
- Son, S., Ryu, J., Lee, N., and Lee, J. The role of masking for efficient supervised knowledge distillation of vision transformers. In *European Conference on Computer Vision*, pp. 379–396. Springer, 2025.
- Sun, S., Cheng, Y., Gan, Z., and Liu, J. Patient knowledge distillation for bert model compression. *arXiv preprint arXiv:1908.09355*, 2019.
- Sun, S., Ren, W., Li, J., Wang, R., and Cao, X. Logit standardization in knowledge distillation. In *Proceedings of the IEEE/CVF Conference on Computer Vision and Pattern Recognition*, pp. 15731–15740, 2024.
- Tang, R., Lu, Y., Liu, L., Mou, L., Vechtomova, O., and Lin, J. Distilling task-specific knowledge from bert into simple neural networks. *arXiv preprint arXiv:1903.12136*, 2019.
- Tian, Y., Krishnan, D., and Isola, P. Contrastive representation distillation. *arXiv preprint arXiv:1910.10699*, 2019.
- Touvron, H., Cord, M., Douze, M., Massa, F., Sablayrolles, A., and Jégou, H. Training data-efficient image transformers & distillation through attention. In *International conference on machine learning*, pp. 10347–10357. PMLR, 2021a.
- Touvron, H., Cord, M., Sablayrolles, A., Synnaeve, G., and Jégou, H. Going deeper with image transformers. In *Proceedings of the IEEE/CVF international conference on computer vision*, pp. 32–42, 2021b.
- Wang, J., Hu, X., Zhang, P., Li, X., Wang, L., Zhang, L., Gao, J., and Liu, Z. Minivlm: A smaller and faster vision-language model. *arXiv preprint arXiv:2012.06946*, 2020.
- Wang, Y., Li, X., Weng, S., Zhang, G., Yue, H., Feng, H., Han, J., and Ding, E. Kd-detr: Knowledge distillation for detection transformer with consistent distillation points sampling. In *Proceedings of the IEEE/CVF Conference on Computer Vision and Pattern Recognition*, pp. 16016–16025, 2024.
- Wightman, R. Pytorch image models. <https://github.com/rwightman/pytorch-image-models>, 2019.
- Xu, K., Rui, L., Li, Y., and Gu, L. Feature normalized knowledge distillation for image classification. In *European conference on computer vision*, pp. 664–680. Springer, 2020.

- Yang, J., Martinez, B., Bulat, A., Tzimiropoulos, G., et al. Knowledge distillation via softmax regression representation learning. *International Conference on Learning Representations (ICLR)*, 2021.
- Yang, Z., Zeng, A., Li, Z., Zhang, T., Yuan, C., and Li, Y. From knowledge distillation to self-knowledge distillation: A unified approach with normalized loss and customized soft labels. In *Proceedings of the IEEE/CVF International Conference on Computer Vision*, pp. 17185–17194, 2023.
- Zagoruyko, S. and Komodakis, N. Paying more attention to attention: Improving the performance of convolutional neural networks via attention transfer. *arXiv preprint arXiv:1612.03928*, 2016.
- Zeng, J., Yang, Z., Yang, Q., Yang, L., and Lin, H. Peeling back the layers: Interpreting the storytelling of vit. In *Proceedings of the 32nd ACM International Conference on Multimedia*, pp. 7298–7306, 2024.
- Zhao, B., Cui, Q., Song, R., Qiu, Y., and Liang, J. Decoupled knowledge distillation. In *Proceedings of the IEEE/CVF Conference on computer vision and pattern recognition*, pp. 11953–11962, 2022.
- Zhou, H., Song, L., Chen, J., Zhou, Y., Wang, G., Yuan, J., and Zhang, Q. Rethinking soft labels for knowledge distillation: A bias-variance tradeoff perspective. *arXiv preprint arXiv:2102.00650*, 2021.

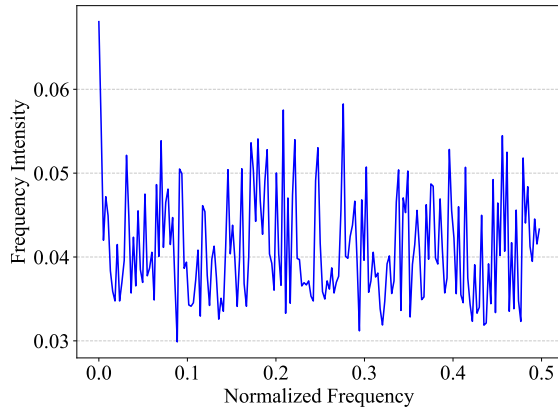
## A. Complete Spectral Distribution Analysis Across All Layers



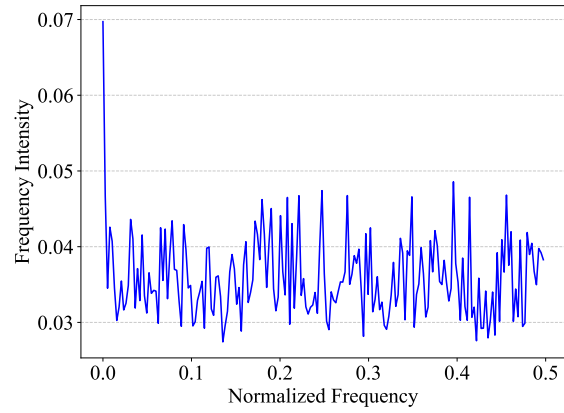
(a) Layer 1.



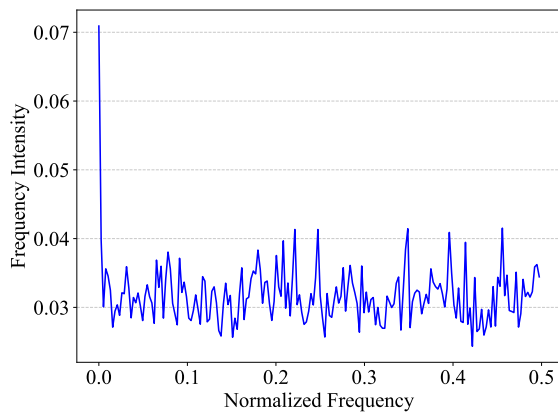
(b) Layer 2.



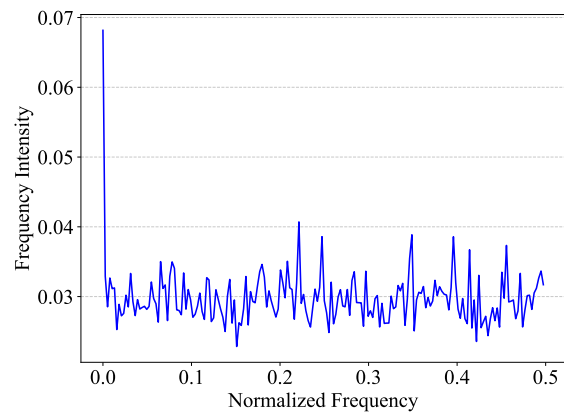
(c) Layer 3.



(d) Layer 4.

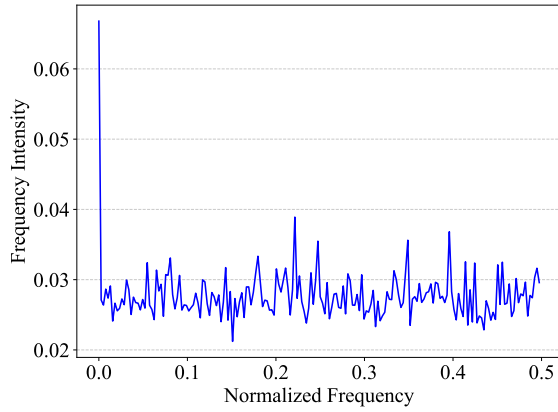


(e) Layer 5.

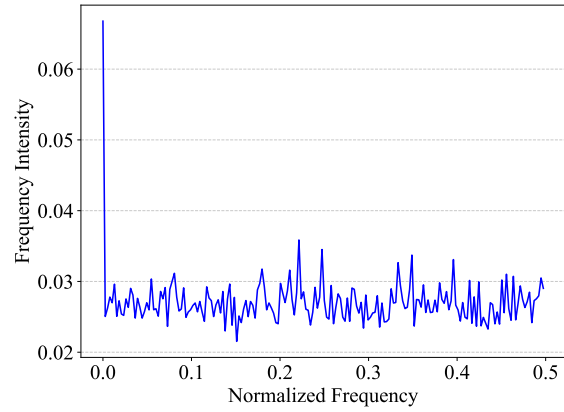


(f) Layer 6.

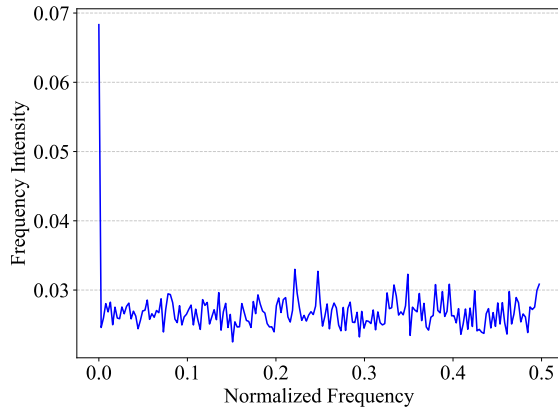
Figure 5. Spectral intensity distributions  $\mathbf{S}(\mathbf{X})$  computed using Equation (3) for layers (1-6) of CaiT-S24 feature maps.



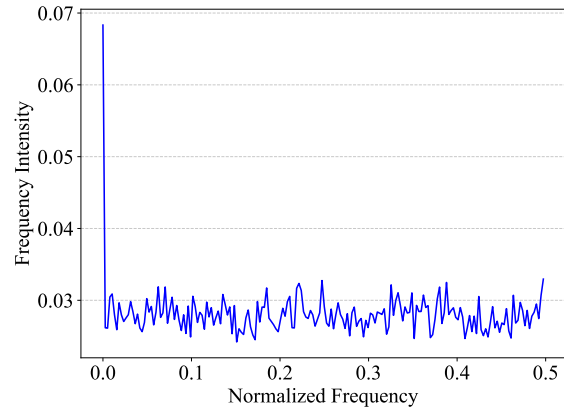
(a) Layer 7.



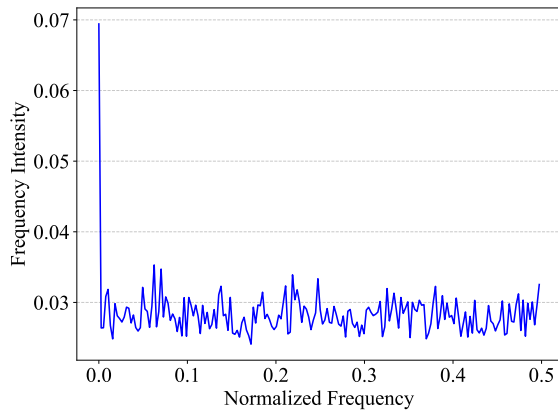
(b) Layer 8.



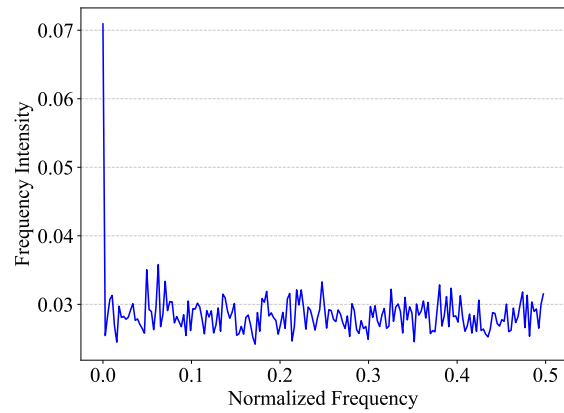
(c) Layer 9.



(d) Layer 10.

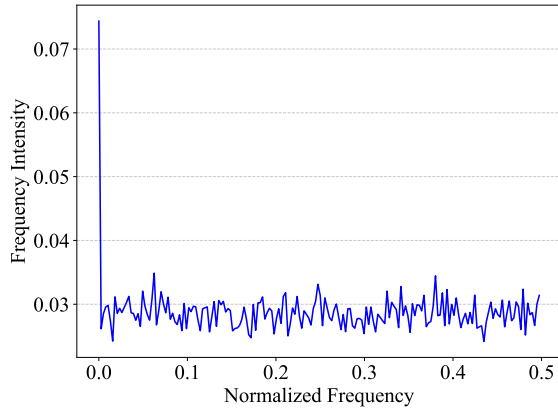


(e) Layer 11.

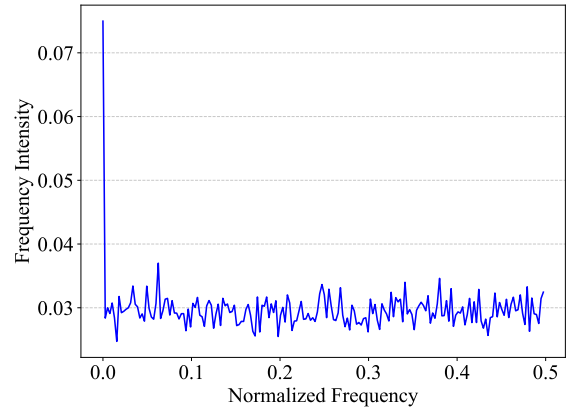


(f) Layer 12.

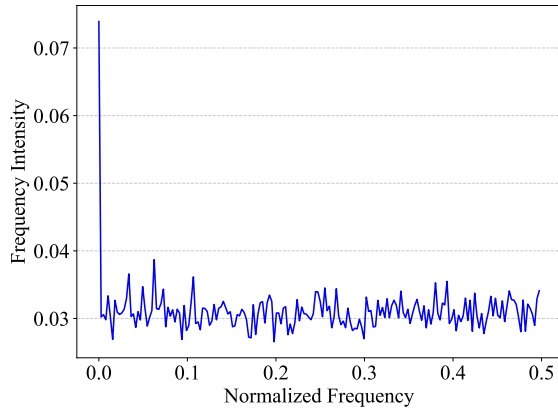
Figure 6. Spectral intensity distributions  $\mathbf{S}(\mathbf{X})$  computed using Equation (3) for layers (7-12) of CaiT-S24 feature maps.



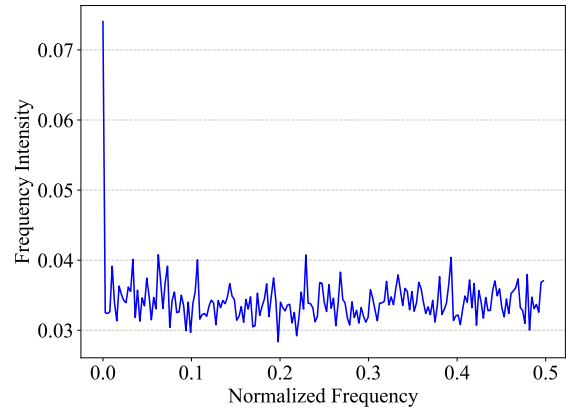
(a) Layer 13.



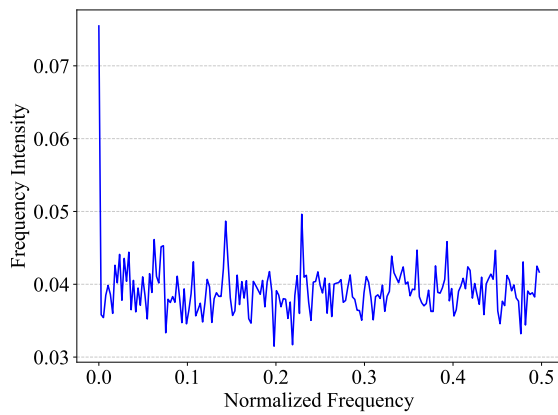
(b) Layer 14.



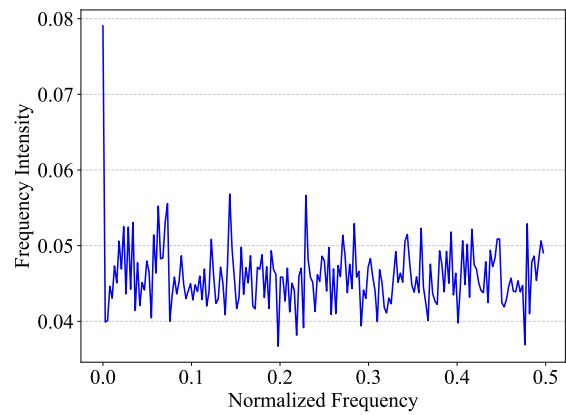
(c) Layer 15.



(d) Layer 16.

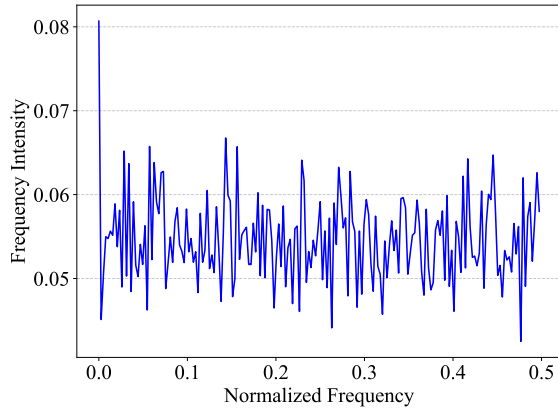


(e) Layer 17.

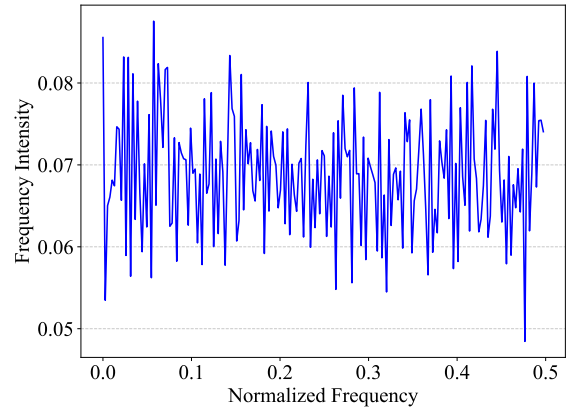


(f) Layer 18.

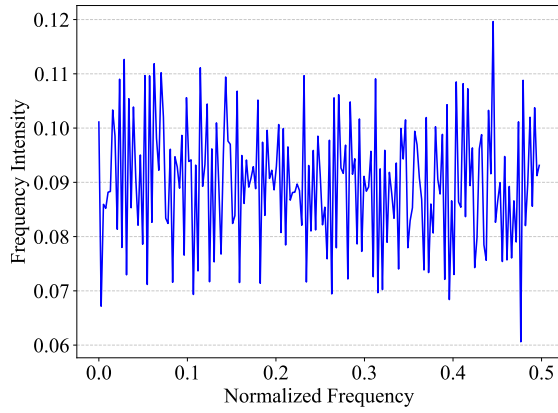
Figure 7. Spectral intensity distributions  $S(\mathbf{X})$  computed using Equation (3) for layers (13-18) of CaiT-S24 feature maps.



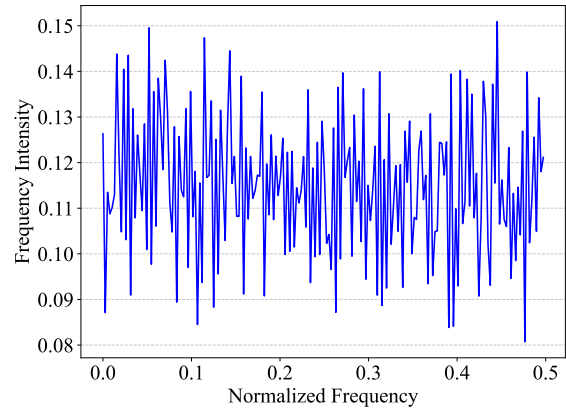
(a) Layer 19.



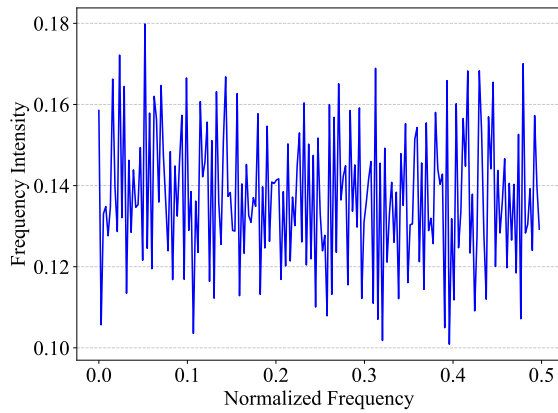
(b) Layer 20.



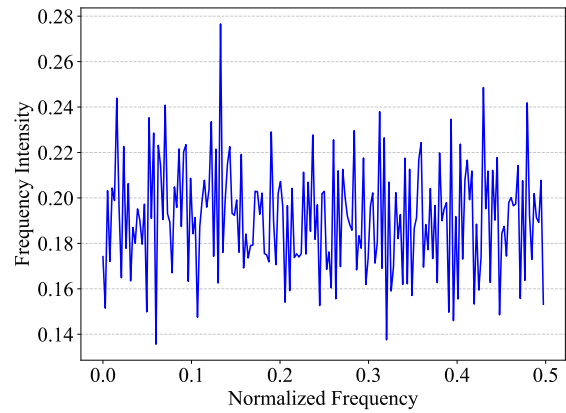
(c) Layer 21.



(d) Layer 22.



(e) Layer 23.



(f) Layer 24.

Figure 8. Spectral intensity distributions  $S(\mathbf{X})$  computed using Equation (3) for layers (19-24) of CaiT-S24 feature maps.